Evaluation of an Advanced Proximity Detection System for Continuous Mining Machines

[1]Christopher Jobes, [2]Jacob Carr and [3]Joseph DuCarme

[1,2]Research Engineer, [3]Research Scientist
The National Institute for Occupational Safety and Health
626 Cochran's Mill Road, Pittsburgh, PA 15236
E-mail: chris.jobes@cdc.hhs.gov, jacob.carr@cdc.hhs.gov, joseph.ducarme@cdc.hhs.gov

Abstract

Researchers at the National Institute for Occupational Safety and Health (NIOSH) are advancing the emerging technology of electromagnetic proximity detection, which provides a promising means of protecting workers around any machinery that presents striking, pinning or entanglement hazards. This technology is particularly applicable to mobile underground mining equipment such as remote-control continuous mining machines, which offer perhaps the most difficult safety challenges in the mining industry. The operators of these machines must maintain constant vigilance to keep themselves and others near the machine safe. Tragically, striking and pinning accidents involving continuous mining machines occur every year causing severe injuries and claiming lives. Proximity detection technology has been effectively implemented for other types of equipment in underground and surface mining as well as in other industries. However, applying this technology to remote-control continuous mining machines presents uniquely difficult challenges. Due to visibility and space limitations, the machine operator must routinely work in very close proximity to the machine. In order to protect miners without preventing them from doing their jobs or causing nuisance alarms, NIOSH is now developing intelligent proximity detection technology. This technology accurately determines worker position relative to the machine and responds by intelligently issuing situation-specific alarms to warn the operator or disabling situation-specific machine functions to protect the operator from machine movements that could result in injury. In this paper, the authors review existing proximity warning technologies, describe ongoing NIOSH research on an intelligent proximity warning system, and summarize

current test results. The NIOSH-developed intelligent system has the potential to have a significant impact on the mining industry by greatly advancing the state-of-the-art in proximity detection technology, leading to increased operator safety, and reducing the frequency of injuries and fatalities.

Introduction

Operating large mobile equipment such as a continuous mining machine (CMM), shown in Figure 1, is a hazardous job that workers perform in underground coal mining operations. Some of the conditions which make this hazardous are the potential for roof falls, the close proximity of large moving machinery, decreased visibility due to low lighting and high dust levels, and high noise levels. In addition to the task of cutting coal from the face, continuous mining machine operators must focus attention on their own position, the location of other crewmembers, and the proximity of the machine to the crew. There are unsafe areas that the remote-control continuous mining machine operators and other workers must avoid. Some areas are clearly defined, such as beyond supported top which is defined by the last row of bolts supporting the roof. Recent NIOSH research by Bartels et al. (2009) identified safe and unsafe zones for the operator near the continuous mining machine. Since the mining environment is dynamic, creating physical barriers to keep operators out of the unsafe zones is not feasible.

Figure 1: Continuous Mining Machine

In the past, operation of continuous mining machines was performed from the machine cab in a seated position. In the 1980s, new technology enabled the transition to remote-control of the mining machinery. By removing the operator from the machine cab, several safety hazards associated with having the operator near the coal face were alleviated. With remote-control capability, the operators are now free to position themselves for better safety and better visibility of the workplace. Typically, the operator positions themselves behind and to one side of the machine during cutting operations. During tramming, the operator walks near the rear of the machine in high coal seams where the machine is less of an obstruction. In low coal seams, the operator trams the continuous mining machine while walking or crawling in front of it. This difference is because the operator cannot see over the machine from the rear. Unfortunately, operators have the tendency to step beside a moving continuous mining machine for a better view during forward, reverse and turning movements while cutting coal or tramming. Bauer et al. (1994) reported that the practice of extended-cut mining has increased the operators' tendency to position themselves in hazardous locations. Additionally, Steiner et al. (1994) stated that an unforeseen consequence of remote-control operation is that an operator can position themselves in dangerous or hazardous locations that could result in a fatality or injury from possible roof falls, mine wall breakouts, pinch-points or other vehicle traffic. Adding to the hazards of operating a continuous mining machine is the restricted workspace with reduced visibility. The mine work environment, such as in low coal seams shown in Figure 2, puts continuous mining machine operators and helpers in awkward work postures for a job consisting of tasks that require fast reactions to avoid being struck by moving equipment. Furthermore, Lewis (1986) reported that restricted visibility due to the nature of the mine environment and low lighting conditions further complicates the tasks involved in operating mining equipment.

Figure 2: Typical Mine Environment

The Mine Safety and Health Administration (MSHA) recommends a set of "red zones" that define dangerous areas near the continuous mining machine, and operators are supposed to avoid these areas. These zones help operators to understand and avoid potentially dangerous areas within the turning radius of the machine. While this concept has been around since the mid 1990's, fatalities and injuries continue to occur with moving machinery underground. A survey of the 2002–2008 accident data from MSHA reveals that an average of 252 accidents occurs per year involving remote-controlled continuous mining machines. Since 1984, there have been 33 fatalities involving workers being struck or pinned by these machines. This indicates that violations of the red zone recommendation occur frequently. Research (Bartels, 2009) shows the red zone guidelines address potentially hazardous situations, but ignore what the operators need to see and sometimes conflict with where the machine operators would like to position themselves in order to perform their job. A technological control to prevent the continuous mining machine from making hazardous motions with workers nearby would reduce the frequency of these accidents. A promising technology for this purpose is electromagnetic proximity detection, which utilizes magnetic fields to determine the proximity of workers to the machine. In this paper, we present an advanced, intelligent system utilizing electromagnetic proximity detection hardware along with novel and efficient software for determining the 2- or 3-dimensional position of a worker and intelligently responding with alarms or disabling machine movement. The implementation of this intelligent system could greatly improve the safety of miners while also reducing the frequency of false alarms that are a problem for some currently available proximity detection systems.

Background

Remote-control operation has required the continuous mining machine operators to divide their attention and process more information simultaneously. Defining and prioritizing what cues and feedback the operator needs and determining what operators focus their attention on can then be used to develop safe, realistic operating procedures. The cues that operators use are primarily visual but will sometimes include auditory information to compensate when visual cues are blocked. Researchers can use this information when analyzing human-machine systems, it is important to examine the components of the mining machine operator and the machine within the work environment. The mining environment is a unique challenge due to its dynamic nature, many hazards, and operational information that must be continually monitored by the continuous mining machine operator. The ability to process and utilize feedback information, in particular the visual cues the operator uses, is an important component of the human-machine system. Safe and effective control of the system is dependent upon the worker properly sensing pertinent information and processing it to make the right decisions. Experienced miners have expanded their knowledge, skills, and abilities to perform safely and effectively. By identifying the specific cues used by these experienced operators, interventions and training methods can be designed to improve safety for all operators.

Previous studies by Bartels et al. (2009) identified and defined visual attention locations (VALs) associated with remote operation of continuous mining machines. In this research, VALs are particular locations needed and visually used by the operator for machine control and operation. The operator needs to consider safe work positions, sounds, vibrations, and operator VALs such as machine orientation, operating characteristics and other visual cues within the work environment to perform their job effectively. These factors have to be accommodated concurrently when considering a safe operator location. The optimum work location for an operator may differ depending on the length of cut, visibility, roof condition, ventilation and avoidance of moving machinery. As part of this research project, the study gathered information on operator work positions and VALs needed when the operator trammed a continuous mining machine during the cutting phase or when moving to a new location. Analysis of the data defined the operators' risk of injury relative to the operators' task, equipment and workplace environment. The results showed that operators of continuous mining machines needed to maintain a 3-foot minimum distance for safety. In addition, the data indicated that a major contributing factor to continuous mining machine related injuries is operators positioning themselves in a hazardous position in order to see cues or VALs.

Several types of proximity detection systems using various technologies have been developed (Ruff and Hession-Kunz 2001; Ruff and Holden 2003; Ruff 2004; Kloos, Guivant et al. 2006; Ruff 2006; Ruff 2007). Some of the technologies utilized in surface mining and in other industries include the Global Positioning System (GPS), and radar-, laser- or ultrasonic-based distance sensors. Unfortunately, these technologies are ineffective in underground mines, where GPS is unavailable, and the constant close proximity of mine walls makes the use of the other sensors extremely difficult.

Another possible solution is the use of Radio Frequency Identification (RFID) technology. Many industries commonly use RFID for tracking the movement of personnel, supplies and equipment. It is also currently in use in the mining industry for tracking the movements of people, equipment and supplies through the mine. These systems are capable of providing information on whether a tag worn by a person or mounted on a machine is within a set range of the transmitter. These systems typically operate in the very-high (VHF) or ultra-high (UHF) radio frequencies, and interference from signal reflections and line-of-sight requirements make applying these systems to continuous mining machines difficult.

Another emerging technology that may be applicable to this problem is intelligent video systems utilizing either single-camera or stereovision and complex algorithms to identify and locate people and machines in the visual scene. However, application of this technology in the underground mining industry is likely to be very challenging due to poor lighting, dust, and the extreme difficulty in keeping the cameras clean.

In a survey of companies implementing proximity detection technology internationally, NIOSH found that mines in South Africa and Australia are using electromagnetic-based systems in several underground coal mining operations. Partnerships between coal operators and the companies marketing the system are a common mechanism for developing these systems. The systems are used on

continuous mining machines as well as other underground equipment such as shuttle cars, roof bolting machines, and feeder/breakers. The systems provide warning and danger zones around equipment. An operator receives visual and audible warnings upon entry into the warning zone and further approach into the danger zone causes the equipment to shut down.

Currently, in the United States, the available systems for underground mining use either magnetic fields or radio frequency technology to alert miners when a machine is close to another machine or a person. On continuous mining machines, these systems will disable all machine movement if an operator moves too close. Recent interviews with the mining community (Kingsley-Westerman, 2010) indicate this action results in frequent nuisance alarms and shut downs. NIOSH researchers are developing technology that adds a measure of intelligence to these systems. The NIOSH intelligent system accurately determines miners' positions relative to the machine and responds by disabling only the specific machine functions that could cause injury.

Intelligent Proximity Detection System

If a proximity detection system is implemented that completely disables machine movement when a person is located near the machine, nuisance alarms are likely to occur frequently. From the standpoint of machine operators, it may seem that the proximity detection system is preventing them from performing their job effectively or standing where they need to stand. For miners to accept the use of proximity detection technology, the technology must provide the necessary protection while minimizing the occurrence of nuisance alarms. NIOSH researchers have developed a solution to this issue in an intelligent proximity detection system. This system accurately determines the position of miners around the continuous mining machine using magnetic fields generated by multiple pulsed electromagnetic field generators. The signal strength from each of these generators is measured by an operator-worn Personal Alarm Device (PAD). Distances are estimated from the signal strengths and are used to triangulate the PAD position. Based on this triangulated position, the onboard controller disables specific machine functions such that unsafe actions are prevented but safe actions are allowed. In this way, the operator maintains the freedom to stand in close proximity to the machine and continue to mine without being hampered by nuisance alarms. The implementation of this technology, along with proper training, is likely to greatly enhance the acceptance of proximity detection by mining machine operators.

An intelligent system of this sort requires a method for accurate position calculation. Therefore, an accurate mathematical model of the magnetic field shape is needed. NIOSH researchers have developed such a model for magnetic field generators that use an antenna with a ferrite rod core typical of proximity detection systems (Carr, Jobes, Li 2010). The shape of the magnetic field is very complex and irregular. Equation (1) defines the shape of the magnetic "shell" in polar coordinates as all points having the same magnetic flux density.

$$\rho = a \cdot cos(2\theta) + b \quad (1)$$

In this equation, ρ is the radial coordinate measured from the center of the magnetic field generator and θ is the angular coordinate measured from the long axis of the magnetic field generator. The coefficients *a* and *b* are functions of the magnetic flux density as defined in (2) and (3).

$$a = c_a \cdot m^{-d_a} \tag{2}$$

$$b = c_b \cdot m^{-d_b} \tag{3}$$

In these equations, m is the magnetic flux density, which decreases with increasing distance from the magnetic field generator, and c_a, d_a, c_b and d_b are all positive constants dependent on the physical and electrical properties of the generator. These constants must be determined through a calibration process for each generator.

Figure 3 shows the magnetic shell shape described by (1). This shell represents all points at which a constant magnetic flux density is measured. Notice that the shell radius varies between ($b + a$) at θ = 0° and 180° and ($b – a$) at 90° and 270° (270° not shown in figure). The shell intersects a circle of radius b at 45°, 135°, 225° and 315° (225° and 315° not shown in figure). Inspection of Equation (1) shows that this will always be the case. It should be clear from examination of Figure 3, that if the value of a is large in relation to b then the shape of the magnetic shell will be more irregular. However, if a is very small in relation to b, the shape of the shell will become more regular, approximating a circle. Referring to (2) and (3), the constants behave in such a way that $0<c_a<c_b$ and that $0\leq d_a\leq d_b<1$. This means that as the magnetic flux density, m, becomes smaller (i.e. the distance from the generator becomes larger), both a and b will increase, but the rate of increase for b will be much faster. This means that as the distance from the generator increases, the shapes of the magnetic shells becomes more regular. The three-dimensional model, shown in Figure 4, is found by the fact that the magnetic field is rotationally symmetric around the θ = 0° axis.

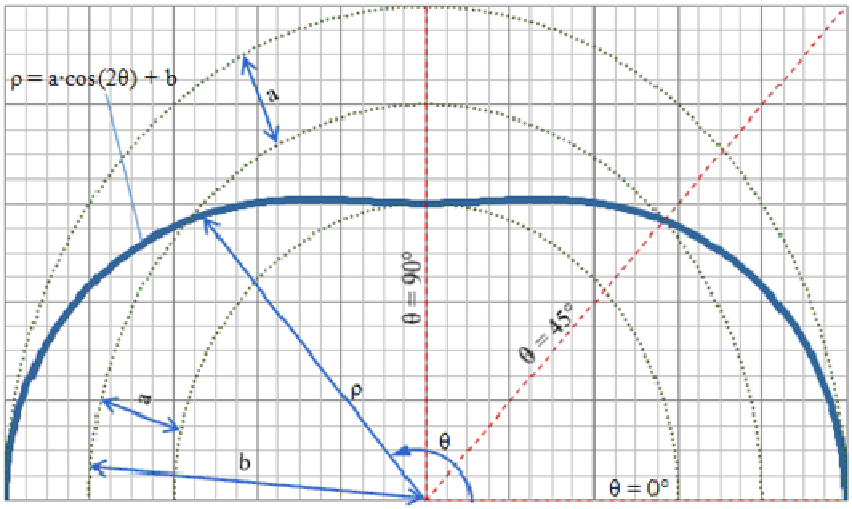

Figure 3: General polar form of magnetic field model for a ferrite-cored generator.

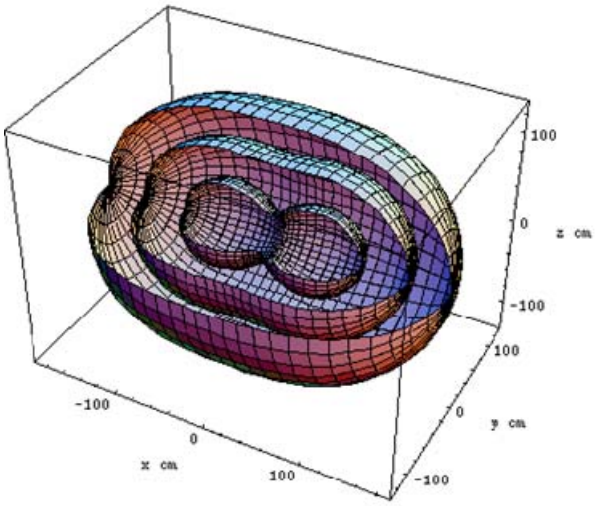

Figure 4: Variation in size and shape of magnetic field in three dimensions

The position of the PAD is determined by finding the intersection of two or more magnetic shells. Due to the irregular shapes of these shells, determining this intersection is not a trivial task, and an analytic solution cannot be determined. For two generators, 0 and 1, each will have its own calibration coefficients, and Equation (1) can be constructed for each generator with θ_0 and θ_1 corresponding to generators 0 and 1, respectively. In the 2-D case, the task is to determine the values of θ_0 and θ_1 that correspond to the intersection. This calculation can be done fairly simply with numeric techniques, such as a Newton-Raphson search. However, in the 3-D case, the problem is further complicated by the introduction of the angles of revolution around the $\theta = 0°$ axis, ψ_0 and ψ_1, which must also be determined and numerical solutions become computationally infeasible. Therefore, a novel geometric search method was developed which iteratively converges on the intersection of two fields in either two or three dimensions. The major benefit of this method is that it does not require significantly more computation time to find solutions in three dimensions. This makes it feasible for use with an onboard processor.

This method converges to the intersection of the shells through an iterative series of spherical approximations. This method, described in three dimensions by Carr et al. (2010), can be most easily visualized in a two-dimensional simplification as shown in Figure 5. In this figure, two generators, 0 and 1, are located in a plane at arbitrary positions, $\bar{\boldsymbol{P}}_{\boldsymbol{0}}$ and $\bar{\boldsymbol{P}}_{\boldsymbol{1}}$, and arbitrary orientations. The solid lines around the generators indicate the magnetic shells defined by Equation (1) in which the angles θ_0 and θ_1 are defined relative to the long axis of generators 0 and 1, respectively. The shells can be approximated by two circles of radius r_0 and r_1. For the first iteration, an initial guess for the radii is made by assuming the average shell radius b as defined in Equation (3). These two circles will intersect at up to two points, $\bar{\boldsymbol{I}}_{\boldsymbol{0}}$ and $\bar{\boldsymbol{I}}_{\boldsymbol{1}}$. From either of these intersections, the angles, θ_0 and θ_1, can be determined through geometry. These angles can then be used with Equation (1) to determine the model shell radii, ρ_0 and

ρ_1. These radii are then used as the new radii, r_0 and r_1, for the circular shell approximations, and the process is repeated. It has been empirically determined that if this process is iterated, and the intersection $\bar{\boldsymbol{I}}_{\boldsymbol{0}}$ is used in every iteration, the solution will quickly converge to the actual intersection, $\bar{\boldsymbol{I}}_{\boldsymbol{0}}^{*}$, of the two shells. Similarly, if $\bar{\boldsymbol{I}}_{\boldsymbol{1}}$ is used, $\bar{\boldsymbol{I}}_{\boldsymbol{1}}^{*}$ will be found. Iteration of the algorithm is halted when the radii, r_0 and r_1, change by an amount less than a preset tolerance in a single iteration.

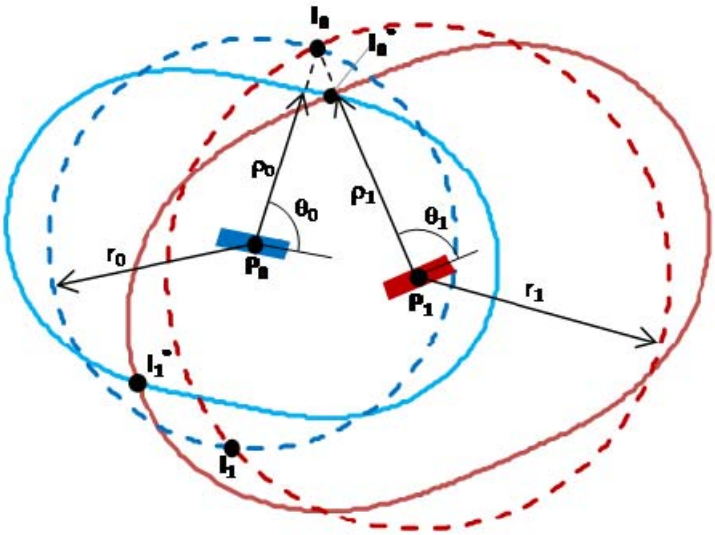

Figure 5: Iterative spherical approximation method in two dimensions

To extend this algorithm to three dimensions, the three-dimensional shells are approximated with spheres, and some additional constraining assumptions are made. It should be clear that an intersection between two three-dimensional shells would be either a point or, more likely, an infinite number of points located on an intersection curve. To limit the possible number of solutions, a further assumption is made that the PAD lies in a plane assumed parallel to and at a specified waist height from the ground surface. Based on the posture of the miner, a reasonably accurate assumption about the PAD elevation can be made. The inaccuracy introduced by having a poor PAD elevation assumption is analyzed in the test results later in this paper.

Once a PAD position has been determined, the next step is to determine which machine functions to disable and which to allow. This is done by defining a number of zones around the machine. For the implementation and testing of the prototype system developed by NIOSH, a set of zones have been defined with associated shutdown logic. However, this is only one possible implementation and is not a recommendation for all mines. The conditions and standard operating procedures at a given mine should be considered when designing the logic that controls the proximity detection system. Figure 6 shows the zones defined for the prototype system and Table 1 shows the machine functions that are disabled for each of these zones. Note that the zones overlap each other and extend over the mining machine itself.

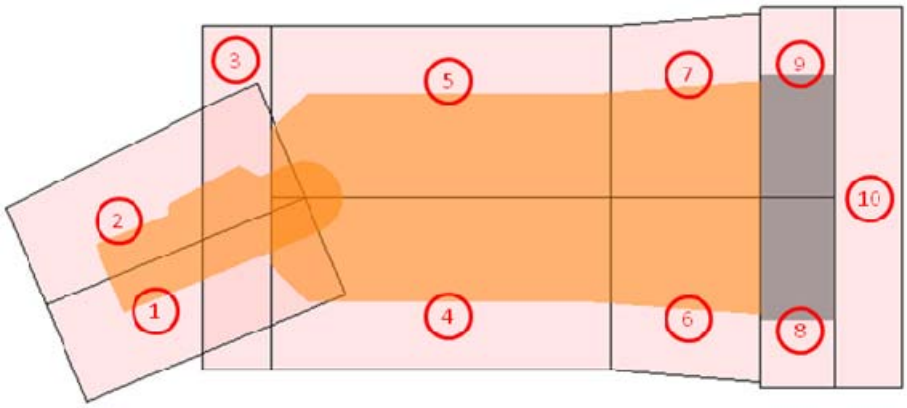

Figure 6: Safety zones used in prototype system.

Table 1: Machine functions disabled by zone

		Zone									
		1	2	3	4	5	6	7	8	9	10
Tram	both forward										X
	right only forward	X			X			X		X	X
	left only forward		X			X	X		X		X
	both reverse	X	X	X							
	right only reverse	X	X	X		X	X		X		
	left only reverse	X	X	X	X			X		X	
	right forward/left reverse	X		X	X			X		X	X
	left forward/right reverse		X	X		X	X		X		X
Conveyor	raise	X	X								
	lower										
	swing right	X									
	swing left		X								
Cutter head	raise								X	X	X
	lower								X	X	X
Gathering pan	raise								X	X	X
	lower								X	X	X
Cutter motor									X	X	X
Conveyor motor		X	X	X							
High speed tram		X	X	X	X	X	X	X	X	X	X

Each zone is defined as a convex polygon with an arbitrary number of sides, N. The vertices of the polygon, $\boldsymbol{v_i}$ (i = 1...N), must lie in the horizontal plane and must be defined in the clockwise direction. The triangulated PAD position is $\boldsymbol{P}$, and the PAD is assumed to be within a circle of radius, r, centered at $\boldsymbol{P}$. The radius, r, corresponds to the uncertainty in the PAD position. Therefore, the task is to determine whether the

polygon defined by $\boldsymbol{v_i}$ (i = 1…N) intersects this circle and if, therefore, the PAD may be within the polygonal zone. Figure 7 shows a general illustration of this problem.

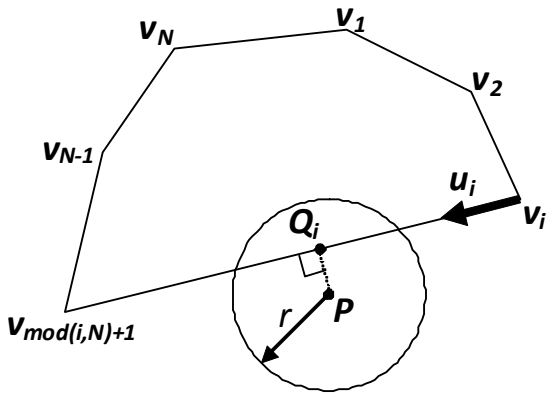

Figure 7: Zone identification algorithm

The first step is to determine whether $\boldsymbol{P}$ is within the polygonal zone. This is done by evaluating Equation 4, in which $\boldsymbol{z}$ is a unit vector in the upward vertical direction, for i = 1…N. If this expression is true for all values of i, then $\boldsymbol{P}$ must be within the zone in question.

$$\left[(\boldsymbol{P}-\boldsymbol{v_i})\times\left(\boldsymbol{v_{mod(i,N)+1}}-\boldsymbol{v_i}\right)\right]\cdot\boldsymbol{z}>0 \tag{4}$$

If this is not true, the next step is to determine whether the circle intersects any of the polygon edges. Each edge is checked individually. To do this, first a unit vector, $\boldsymbol{u}$, is defined pointing from $\mathbf{v_i}$ to $\mathbf{v_{mod(i,N)+1}}$ by Equation (5).

$$\boldsymbol{u_i}=\frac{\boldsymbol{v_{mod(i,N)+1}}-\boldsymbol{v_i}}{\left\|\boldsymbol{v_{mod(i,N)+1}}-\boldsymbol{v_i}\right\|} \tag{5}$$

This unit vector is used in Equation 6 to find a point, $\boldsymbol{Q_i}$ which is the closest point to $\boldsymbol{P}$ on the polygon edge.

$$\boldsymbol{Q_i}=min\left(max\left((\boldsymbol{P}-\boldsymbol{v_i})\cdot\boldsymbol{u_i},0\right),\left\|\boldsymbol{v_{mod(i,N)+1}}-\boldsymbol{v_i}\right\|\right)\boldsymbol{u_i}+\boldsymbol{v_i} \tag{6}$$

Finally, if Equation 7 is true for any value of i, the circle centered at $\boldsymbol{P}$ must intersect the polygonal zone.

$$\|(\boldsymbol{P}-\boldsymbol{Q_i})\|\leq r \tag{7}$$

If Equation 4 is true for all values of i or if Equation 7 is true for any value of i, the PAD is located within the zone. This is repeated for all zones. Because the zones can overlap, and because the PAD position is defined as a circle rather than as a single point, it is possible for the PAD to be located in more than one zone. In this case, only those machine functions that are allowed in all zones in which the PAD is located will be allowed.

Test Procedures

This system has been implemented and tested using a Joy 14CM continuous mining machine as a prototype platform. The installed proximity detection hardware is shown in Figure 8, and the host PC used for programming and testing is shown in Figure 9. Figure 10 illustrates, conceptually, the interface between the intelligent proximity detection system and the mining machine control hardware. Normally, the remote control sends operator input to the demultiplexer (or demux) which sends control signals to the individual actuators. In the prototype system, the actuator signals travel through a set of relays that the onboard controller selectively opens or closes. In this manner, individual controls are selectively disabled, but the software does not send active control signals to the actuators. This implementation was effective for the prototype system, but is only one of several types of hardware that could achieve similar behavior. Figure 11 shows the major components installed on the Joy 14CM.

Figure 8: Electromagnetic PAD and field generator used for prototype system.

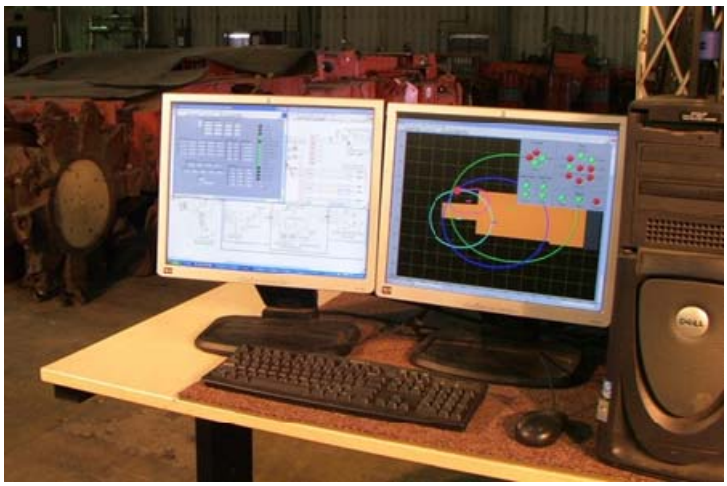

Figure 9: Host PC used for programming and testing prototype system.

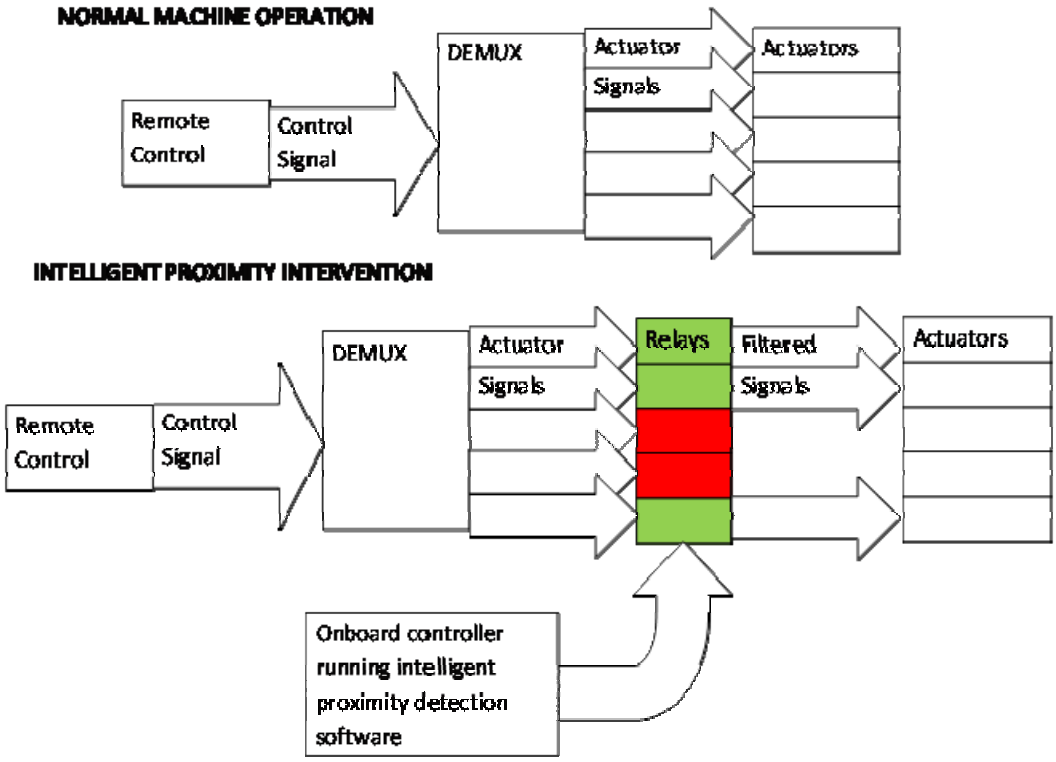

Figure 10: Relay-based hardware implementation

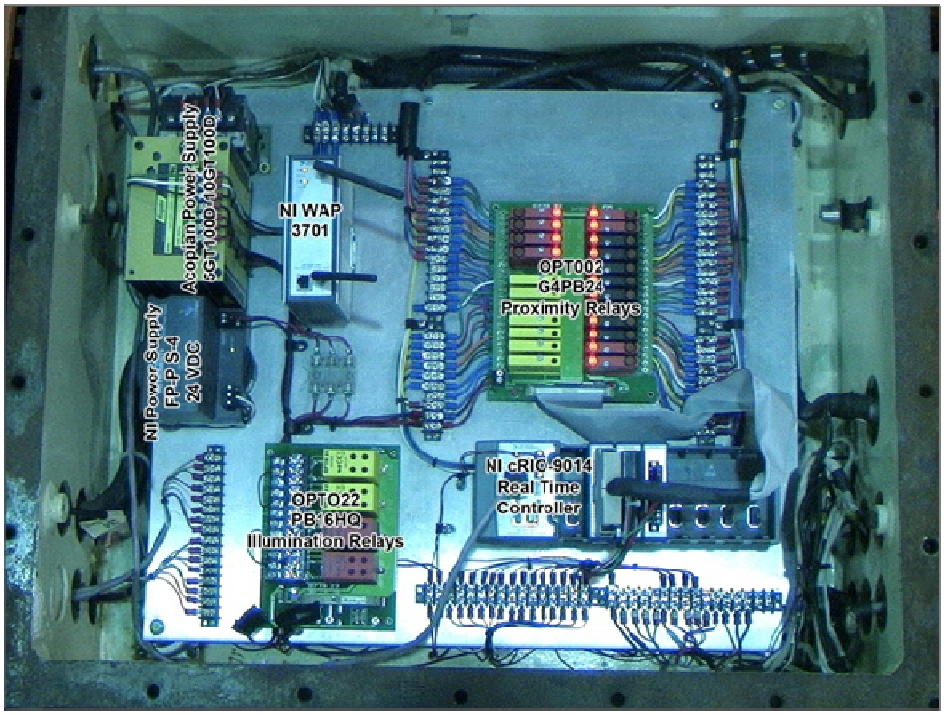

Figure 11: Intelligent control hardware as installed on Joy 14CM prototype testbed

The generator placement in the prototype system was designed to provide excellent triangulation accuracy near the mining machine. With the available hardware it was impossible to provide coverage around the entire machine. The generators were concentrated near the rear of the mining machine since this is where the operator usually stands. The generator placement is shown in Figure 12. Planned future work will expand the prototype system to extend coverage over the entire machine.

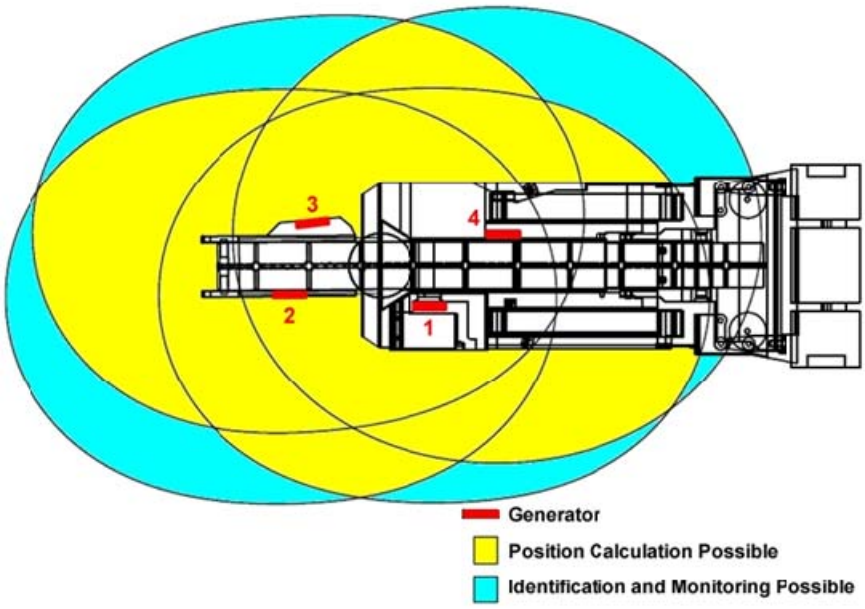

Figure 12: Generator placement in prototype system; generators concentrated near rear of the machine due to range limitations

The model given in Equations 1-3 was calibrated using measurements taken with a PAD at various locations around each of the generators. From these measurements, a least-squares fit was used to determine the model coefficients for each generator. For this prototype installation, these coefficients are summarized in Table 2. These coefficients provide the radius, ρ, based on the magnetic field strength reading received from the proximity hardware, which is proportional to the magnetic flux density.

Table 2: Model calibration coefficients used for prototype tests.

	Generator 1	**Generator 2**	**Generator 3**	**Generator 4**
c_a	104.6	45.6	32.1	159.6
d_a	-0.210	0	0	-0.322
c_b	1287.5	977.0	1883.4	1696.7
d_b	-0.264	-0.211	-0.340	-0.322

Using this calibration, the accuracy and reliability of the prototype intelligent proximity detection system has been tested. The accuracy is measured as the distance between the actual PAD position and the triangulated position. Since the accuracy is critical within three feet of the machine, the prototype system has been designed to have excellent accuracy in this zone. Therefore, the accuracy has been analyzed in two populations: within three feet of the machine, and outside three feet of the machine.

While the accuracy of the triangulation gives an indication of the system performance, a more important measure is the reliability with which the system correctly disables machine movement or issues alarms. Tests were performed to measure this reliability in terms of missed alarms and false alarms. The current implementation of the prototype system does not include visual or audible alarms, so the missed alarm and false alarm rates will be discussed in terms of the machine functions that are disabled by the system. If the PAD is located within a zone as in Figure 6, the machine functions associated with that zone, shown in Table 1 should be disabled. A missed alarm is defined as when a function should have been disabled, but was not. A false alarm is defined as when a function should not have been disabled, but was.

This is slightly complicated when either the actual position or the triangulated position of the PAD is near the boundary of a zone because the position of the PAD is not defined as a single point, but rather as a circle of a particular uncertainty radius. Figure 13 demonstrates several possible scenarios and how they are interpreted. In this figure, the actual and triangulated PAD positions are shown along with the circle associated with the uncertainty. If the actual PAD position is outside but within the uncertainty radius from the zone boundary, it is not clear whether the machine functions associated with that zone should be disabled. In this case, either disabling or not disabling those functions would be considered correct system behavior as this uncertainty is part of the logic design. If the PAD is outside the zone by a distance of more than the uncertainty radius, than a false alarm can occur if the triangulated position is either within or near the zone boundary. A missed alarm only occurs when the actual PAD position is inside the zone and the triangulated PAD position is outside the zone boundary by more than the uncertainty radius.

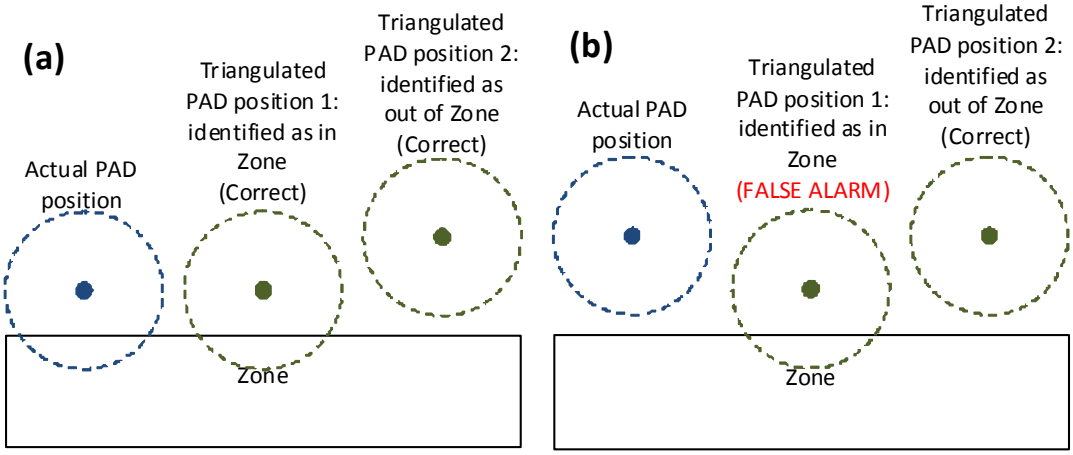

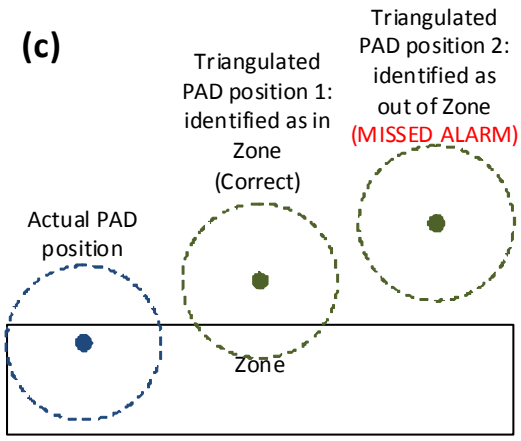

Figure 13: Missed alarm and false alarm logic for cases in which (a) PAD is outside but near the zone, (b) PAD is outside the zone and (c) PAD is inside the zone

Since the PAD can be identified as being within multiple zones, and since some of the zones result in the disabling of the same machine functions, the missed alarm and false alarm rates must be analyzed in terms of the machine functions that are disabled. Consider the case that the PAD is actually located only in zone A, but is identified as being located only in zone B. If a given machine function is disabled for both zones A and B, a missed alarm will not have occurred for that function.

The PAD was mounted on a nonmetallic stand and positioned at all points on a 1-meter grid around the Joy 14CM (Figure 14 and Figure 15). The actual position of the PAD was determined with surveying equipment. Two reference points on the mining machine were located to establish the position and orientation of the machine. This allowed each surveyed location of the PAD to be expressed relative to the mining machine and in the same coordinate system that the proximity detection system uses.

The PAD was positioned at two belt heights: 16 inches, corresponding to a 5^{th} percentile female kneeling, and 46 inches, corresponding to a 50^{th} percentile male standing. In the discussion that follows, these PAD heights are referred to as "low" and "high," respectively. In addition to the actual PAD elevation, the PAD elevation that was assumed by the triangulation software was also varied between the low and high elevations. The tail of the mining machine, which can be moved through a range of 90° in swing and 6° in elevation, was also varied. The swing positions used were left (45° left of center), center (aligned with the machine's centerline) and right (45° right of center). The tail elevation was varied between down (3° above horizontal) and down (9° above horizontal).

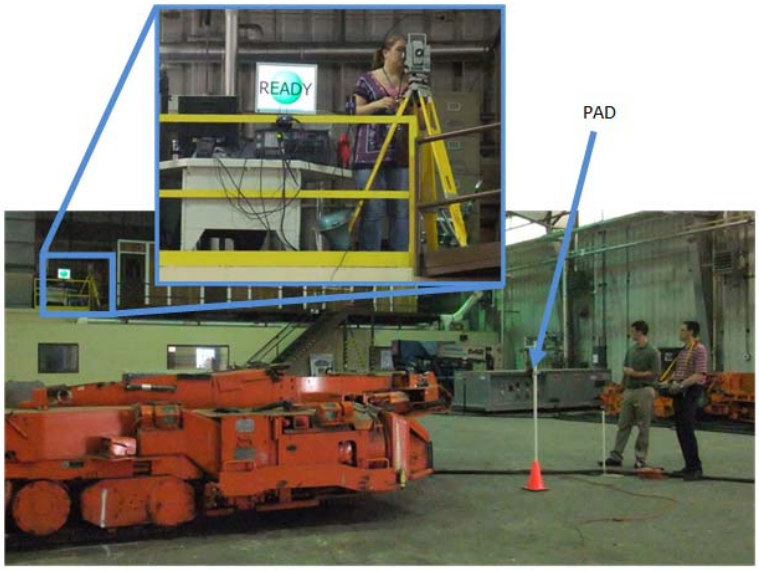

Figure 14: Triangulation accuracy test setup for prototype system

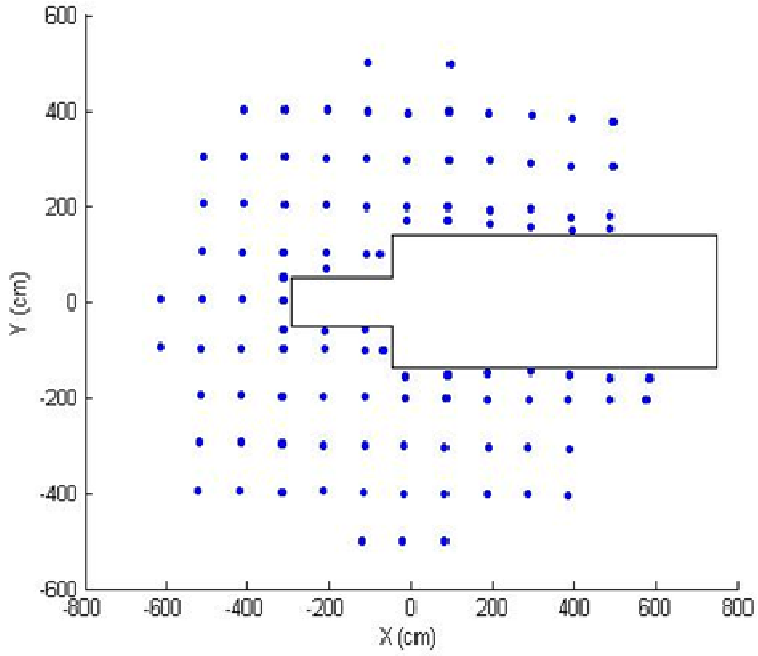

Figure 15: Data collection points.

Test Results

Figure 16 shows the accuracy of the triangulated position for the tests in which the prototype system was installed on the Joy 14CM mining machine. In this figure, the actual position of the PAD is shown with a blue dot and the triangulated position of

the PAD is shown with a green circle. The radius of this circle indicates the 50 cm uncertainty radius used in determining the zone in which the PAD is located. The points for which the system has a missed alarm are highlighted in this figure in red.

Excellent accuracy is achieved close to the machine and the PAD position is generally known to within 20 to 50cm. The errors increase with distance from the generators, tend to be high in specific areas due to generator pair selection for triangulation, and tend to be in a tangential direction due to the shape of the fields. Further from the mining machine, the accuracy is worse, even exceeding 3 meters. However, it can be argued that accuracy further from the machine is not as critical since the miner operator will be in a safer location and only identifying his general location is of importance.

There is a very low occurrence of missed alarms. In the example shown, there is only one missed alarm highlighted in red. In this case, the PAD is actually located very close to the border of one zone, but is determined to be in the adjacent zone. The very large error at this point is because the PAD is located very far from the generators which were concentrated near the rear of the mining machine.

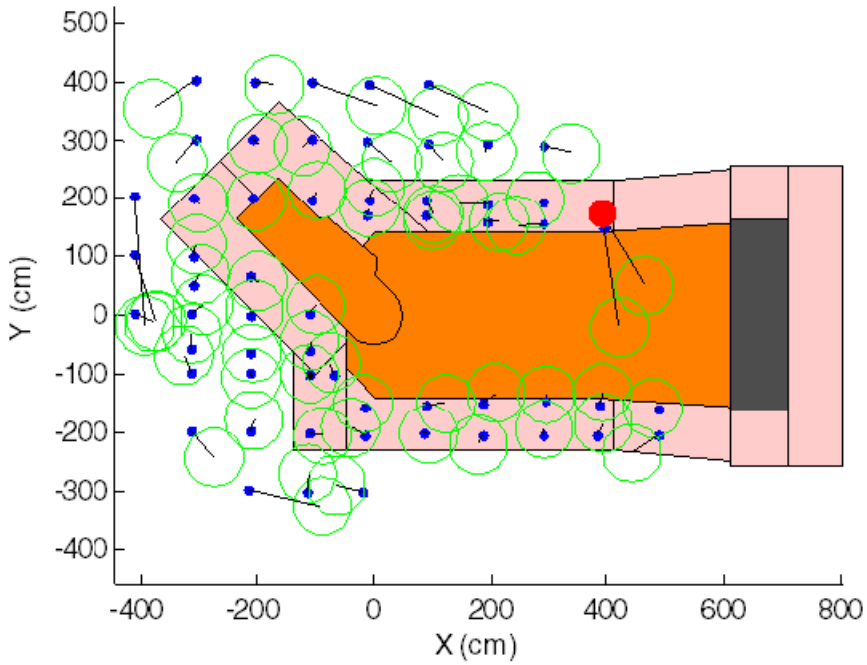

Figure 16: Example triangulation accuracy results with prototype system; dots represent the actual PAD position, circles represent the triangulated PAD position with uncertainty radius, larger solid circle indicates a missed alarm

Figure 17 and Figure 18 summarize the triangulation accuracy achieved in tests with the prototype system. Due to the sampling locations and low sampling density in the prototype system test, the area outside three feet from the machine is somewhat under-represented in these results. The accuracy depends strongly on accurate

knowledge of the PAD elevation. The PAD elevation is needed as a constraint in the triangulation algorithm, and can be assumed based on the posture of the miner. Cases b and c in Figure 17 show how the accuracy can be greatly reduced when a poor estimate of the PAD elevation is used. In general, the accuracy of the triangulation is generally known to within 50 cm for the normal operating case in which the PAD is located at a high elevation and assumed at a high elevation.

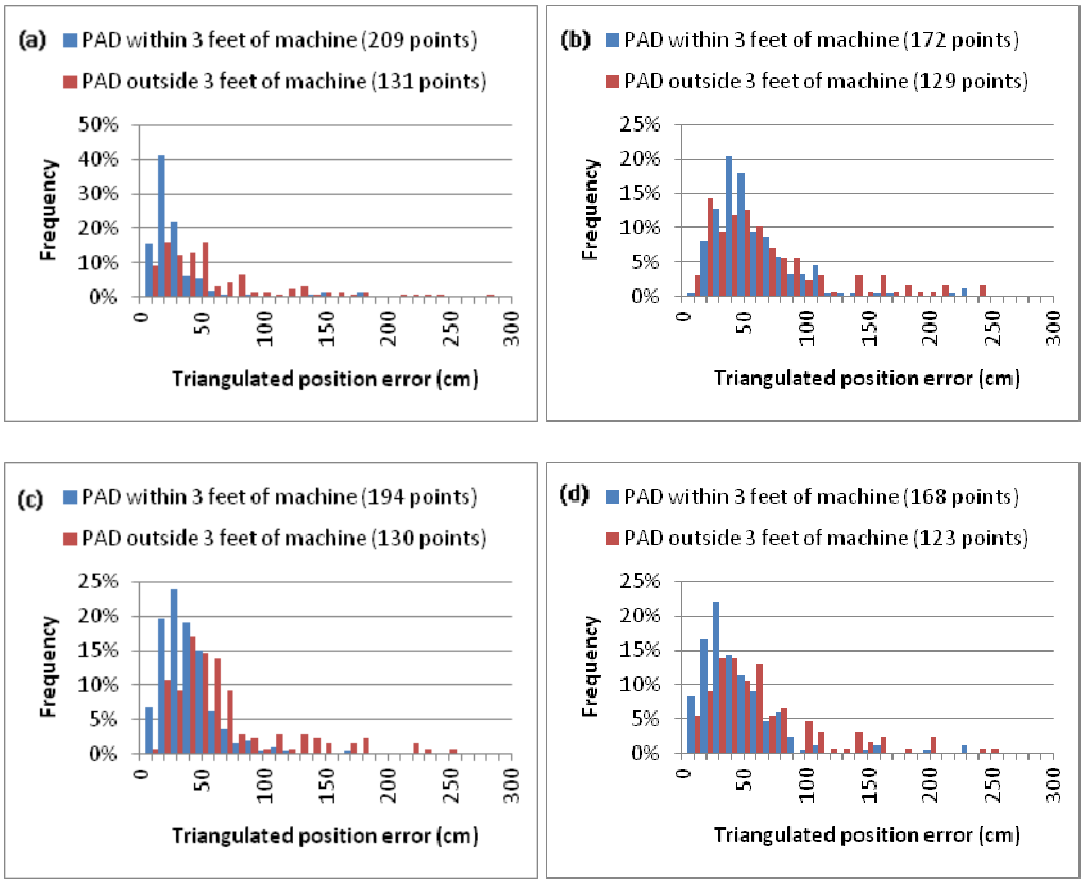

Figure 17: Results of testing with prototype system: PAD position triangulation accuracy for (a) PAD elevation high and assumed high, (b) PAD elevation low and assumed high, (c) PAD elevation high and assumed low, and (d) PAD elevation low and assumed low

PAD within 3 feet of machine							
Assumed PAD Elevation	**Actual PAD Elevation**	**No. of Samples**	**Mean Error (cm)**	**St. Dev. Error (cm)**	**90% Confidence (cm)***	**95% Confidence (cm)***	**Plot symbol**
High	High	209	27	31	48	81	
	Low	172	53	36	93	107	
Low	High	194	34	22	57	72	
	Low	168	41	36	76	84	
PAD outside 3 feet of machine							

Assumed PAD Elevation	Actual PAD Elevation	No. of Samples	Mean Error (cm)	St. Dev. Error (cm)	90% Confidence (cm)*	95% Confidence (cm)*	Plot symbol
High	High	131	56	53	127	163	
	Low	127	64	51	143	174	
Low	High	130	64	52	137	170	
	Low	123	61	50	136	155	

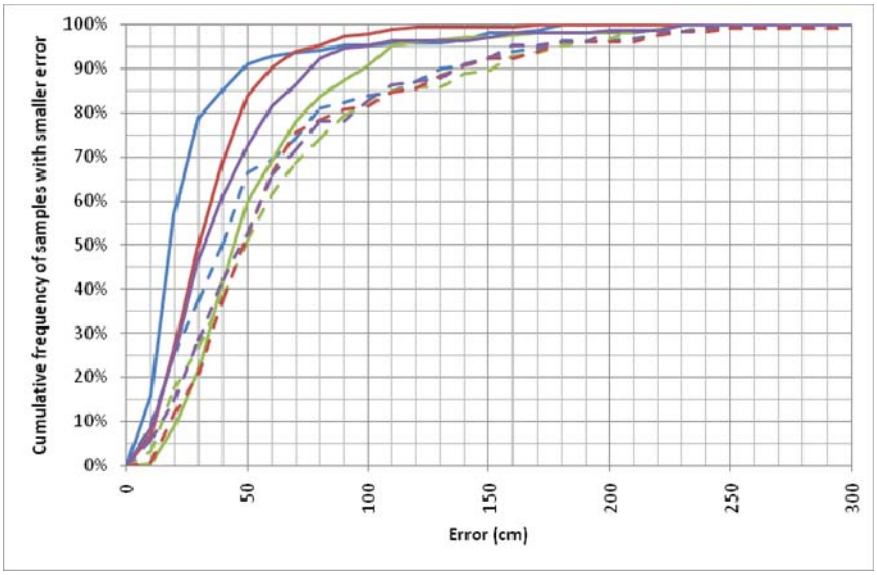

Figure 18: Triangulation accuracy for tests with prototype system represented with cumulative frequency plot

Table 3 summarizes the missed alarm and false alarm rate for the prototype system tests. The "Desired Disable Events" refers to the total number of times any machine function should have been disabled and was determined based on the actual PAD position. The table shows that, in general, the system responds correctly nearly all of the time by disabling the correct machine functions to prevent collisions and allowing those functions that will not cause a collision. In general, the missed alarm rate is low. The missed alarm rate is higher, however, when the PAD is low and the tail is raised. An increase in error is expected in this case because the distance between the generators and the PAD is increased.

In general, however, the results of these tests are very encouraging, showing that under most operating conditions, the system will respond appropriately by disabling the correct machine movements to prevent a collision.

Table 3: System reliability in terms of missed and false alarms as tested with the prototype system

Assumed PAD Elevation	Actual PAD Elevation	Tail Elevation	Tail Swing	Desired Disable Events	Correctly Disabled	Missed Alarms	False Alarms
High	High	Down	Left	194	98.5%	1.5%	21.1%
			Center	233	98.7%	1.3%	13.7%
			Right	215	98.6%	1.4%	33.0%
		Up	Left	190	95.3%	4.7%	10.5%
			Center	233	100.0%	0.0%	11.6%
			Right	202	100.0%	0.0%	23.8%
	Low	Down	Left	178	100.0%	0.0%	10.7%
			Center	199	100.0%	0.0%	6.5%
			Right	187	100.0%	0.0%	16.0%
		Up	Left	174	89.7%	10.3%	8.6%
			Center	201	98.5%	1.5%	8.0%
			Right	174	82.8%	17.2%	4.6%
Low	High	Down	Left	186	100.0%	0.0%	40.9%
			Center	225	100.0%	0.0%	28.0%
			Right	199	100.0%	0.0%	25.1%
		Up	Left	164	100.0%	0.0%	37.8%
			Center	229	100.0%	0.0%	33.6%
			Right	189	100.0%	0.0%	26.5%
	Low	Down	Left	174	100.0%	0.0%	29.9%
			Center	190	100.0%	0.0%	25.8%
			Right	187	95.2%	4.8%	28.3%
		Up	Left	170	89.4%	10.6%	23.5%
			Center	201	100.0%	0.0%	15.9%
			Right	165	87.3%	12.7%	21.2%

Discussion and Future Work

While this prototype system represents a significant advance in the technology of proximity detection and is expected to greatly improve the safety of underground coal miners, more can be done to improve the system's range, reliability, and accuracy. The next step in this research is to expand the number of generators to 6 and enhance their individual range as well so that the entire machine and much of its immediate surroundings can be covered (see Figure 19) Future tests on the resulting system will include quantifying the triangulation accuracy and the system reliability. Simulated mining tasks will be performed to collect data on the human machine interaction aspects of implementing this advanced proximity detection system. NIOSH researchers are also considering using operator worn MEMS inertial sensors to identify the operator posture and thus fine tune the assumed PAD height to improve

triangulation results. Posture information can also be used to make changes on the fly to how the onboard controller reacts to potentially risky control requests by the operator. It is hoped that this new system and/or the technological advances represented in it will be adopted by the industry, and offer improved safety for underground coal miners.

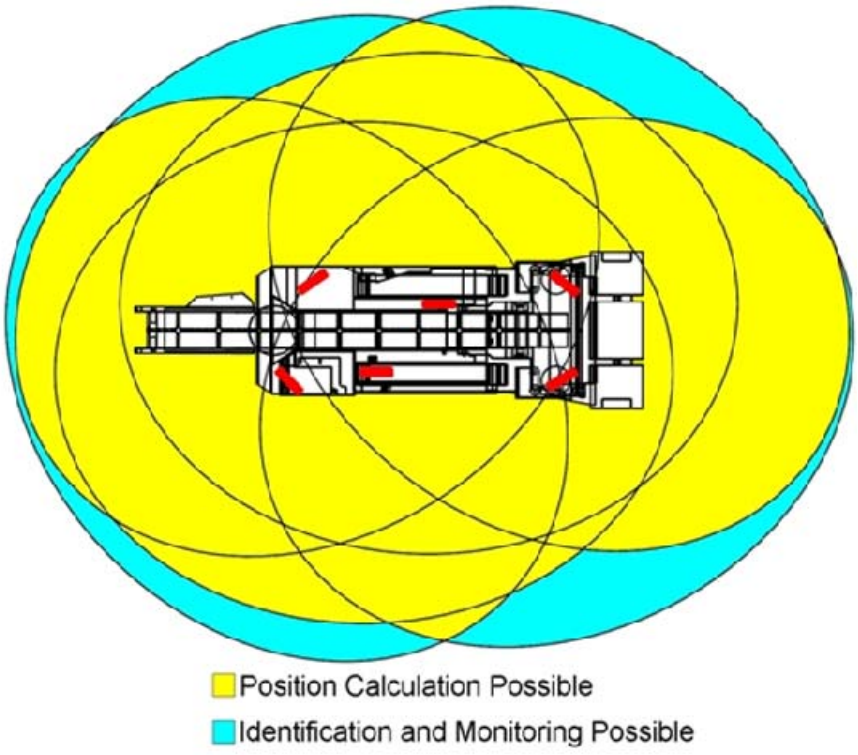

Figure 19: Future 6 generator system allowing coverage of the entire CMM

Disclaimer

The findings and conclusions in this report are those of the authors and do not necessarily represent the views of the National Institute for Occupational Safety and Health.

References

[1] Bartels, J. et al. (2009). Continuous mining: a pilot study of the role of visual attention locations and work position in underground coal mines. Professional Safety 2009 Aug; 54(8):28-35

[2] Bauer, E. et al. (1994). Ground Control Safety Analysis of Extended Cut Mining. Bureau of Mines IC 9372, 24pp.

[3] Carr, J., Jobes, C., Li, J. (2010). Development of a Method to Determine Operator Location using Electromagnetic Proximity Detection. IEEE Robotics and Sensors Environments Conference, Phoenix, AZ, 15-16 Oct. 2010.
[4] Kingsley-Westernan, C. (2010). Behavioral Considerations for Proximity Warning Implementation. Presented at the Proximity Warning Systems for Mining Equipment NIOSH Workshop, Charleston, WV, Sep. 15, 2010.
[5] Kloos, G., Guivant, J., et al. (2006). Range Based Localization Using RF and the Application to Mining Safety. 2006 IEEE/RSJ International Conference, 9-15 Oct. 2006, 1304-1311.
[6] Lewis, W. (1986). Underground Coal Mine Lighting Handbook. Bureau of Mines IC 9073, 42pp.
[7] Ruff, T., Hession-Kunz, D. (2001). Application of radio-frequency identification systems to collision avoidance in metal/nonmetal mines. IEEE Transactions on Industry Applications, 2001 Jan-Feb; 37(1):112-116
[8] Ruff, T., Holden, T. (2003). Preventing collisions involving surface mining equipment: a GPS-based approach. Journal of Safety Research, 2003 Apr; 34(2):175-181
[9] Ruff, T. (2004). Evaluation of devices to prevent construction equipment backing incidents. SAE Technical Paper Series. Commercial Vehicle Engineering Congress and Exhibition, Rosemont, Illinois, 2004-01-2725
[10] Ruff, T. (2006). Evaluation of a radar-based proximity warning system for off-highway dump trucks. Accident Analysis and Prevention, 2006 Jan; 38(1):92-98
[11] Ruff, T. (2007). Recommendations for evaluating & implementing proximity warning systems on surface mining equipment. NIOSH 2007-146; RI-9672
Steiner, L. et al. (1994). Ergonomics of Low Seam Teleoperated Mining. The Second International Symposium on Mine Mechanization and Automation.a